Nitrocellulose Catalyzed With Manganese Oxide Nanoparticles: Advanced Energetic Nanocomposite With Superior Decomposition Kinetics

Sherif Elbasuney (sherif_basuney2000@yahoo.com)
Military Technical College
M. Yehia
Military Technical College
Shukri Ismael
Military Technical College
Yasser El-Shaer
Arab Academy for Science and Technology
Ahmed Saleh
Science and Technology Center of Excellence

Research Article

Keywords: Nanoparticles, Thermites, Hydrothermal synthesis, Energetic materials, Pyrotechnics, First-fire

Posted Date: March 22nd, 2021

DOI: https://doi.org/10.21203/rs.3.rs-311803/v1

Catalyzed Nitrocellulose Nanocomposite: a Novel Energetic Composition with Superior Decomposition Kinetics for Advanced Microchips

Sherif Elbasuney [a,b*], M. Yehia [a], Shukri Ismael [a] , Yasser El-Shaer [c], Ahmed Saleh [d]

[a] School of Chemical Engineering, Military Technical College, Cairo, Egypt.

[b] Head of Nanotechnology Research Center, Military Technical College, Cairo, Egypt.

[C] Mechanical Engineering Department, Arab Academy for Science and Technology.

[d] Science and Technology Center of Excellence, Cairo, Egypt.

*Corresponding: s.elbasuney@mtc.edu.eg, sherif_basuney2000@yahoo.com

Abstract

Nanostructured energetic materials can fit with advanced energetic first-fire, and electric bridges (microchips). Manganese oxide, with active surface sites (negatively charged surface oxygen, and hydroxyl groups) can experience superior catalytic activity. Manganese oxide could boost decomposition enthalpy, ignitability, and propagation rate. Furthermore manganese oxide could induce vigorous thermite reaction with aluminium particles. Hot solid or liquid particles are desirable for first-fire compositions. This study reports on the facile fabrication of MnO_2 nanoparticles of 10 nm average particle size; aluminium nanoplates of 100 nm average particle size were employed. Nitrocellulose (NC) was adopted as energetic polymeric binder. MnO_2/Al particles were integrated into NC matrix via co-precipitation technique. Nanothermite particles offered an increase in NC decomposition enthalpy by 150 % using DSC; ignition temperature was decreased by 8 ^{0}C. Nanothemrite particles offered enhanced propagation index by 261 %. Kinetic study demonstrated that nanothermite particles experienced drastic decrease in NC activation energy by - 42, and - 40 KJ mol^{-1} using Kissinger and KAS models respectively. This study shaded the light on novel nanostructured energetic composition, with superior combustion enthalpy, propagation rate, and activation energy.

Keywords: Nanoparticles; Thermites; Hydrothermal synthesis; Energetic materials; Pyrotechnics; First-fire.

1. Introduction

Nanostructured energetic materials can offer interesting characteristics in terms of high heat output, high reaction rate, as well as controlled sensitivity [1-3]. Nanothermite (metal oxide/metal) can act as efficient high energy dense material, with high volumetric energy density compared with common explosives. Nanothermites can experience reaction rate 100 times compared with conventional counterparts [4-6]. Much research has been directed to the development of nanothermites for initiation means, propulsion, micro-actuator, and electric match compositions [4, 7-8]. Electric match includes a thin metal wire (bridge wire) coated with a dab of heat-sensitive pyrotechnic composition [9]. Hot solid or liquid particles are desirable for first-fire compositions. Reactive fuel particles such as aluminium can produce good heat output and hot solid particulates. Nanothermite particles (metal oxide/metal) are emerging class of high energy density materials. Nanothermites can enhance not only the heat output, but also the ignitability, thermal conductivity, and propagation rate [10]. Manganese oxide is one of the most effective oxidizers for nanothermite reactions. Furthermore MnO_2 has the potentials for catalytic decomposition of energetic materials. Low co-ordination surface oxygen atoms are negatively charged; they have the potential to act as electron donor to electron deficient explosive material [11]. Hydroxyl surface groups could be evolved at low temperature and could attack the NC cyclic ring with the release of active NO_2 [4, 12]. MnO_2 particles could induce condensed phase reaction of gaseous products with the increase in decomposition enthalpy (Figure 1) [13-15].

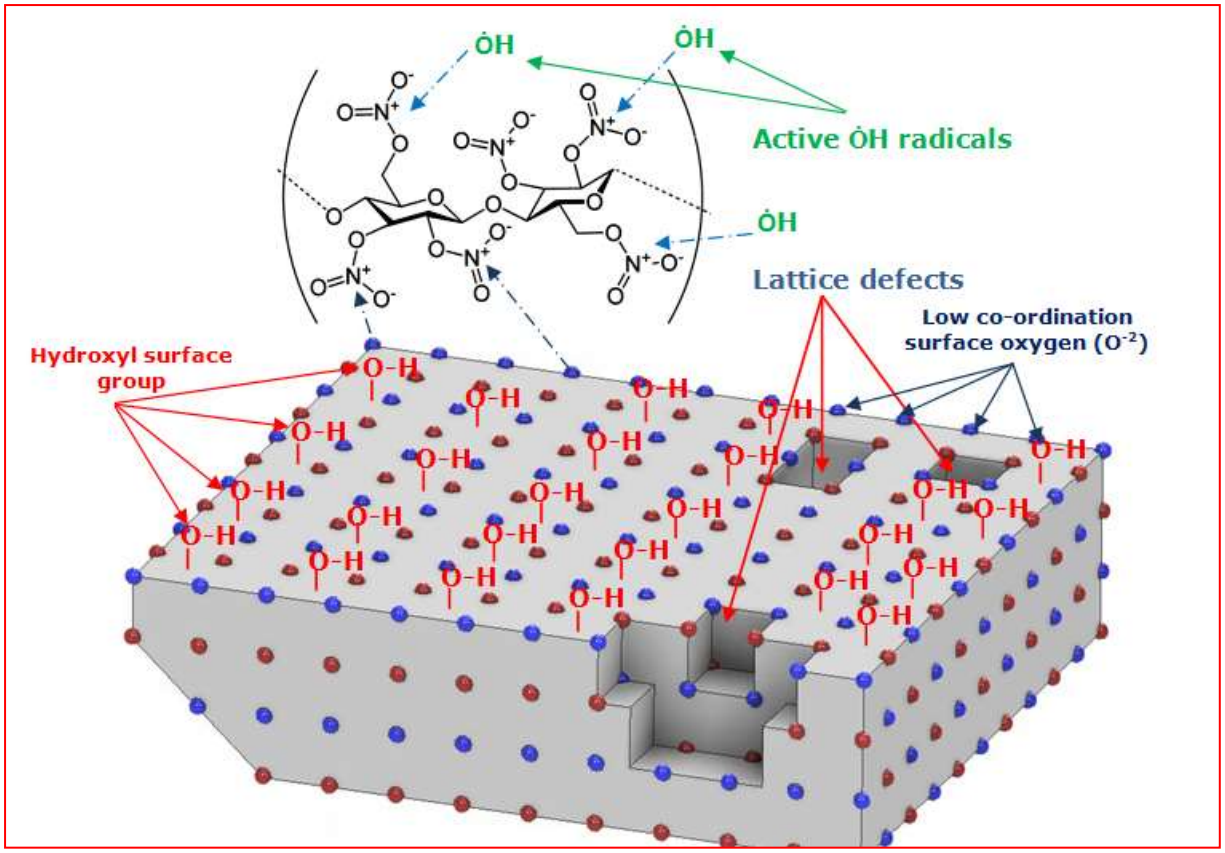

Fig. 1: Schematic for active surface sites of manganese oxide catalyst (i. e. negative surface oxygen, and hydroxyl groups).

On the other hand aluminium can experience decomposition enthalpy of 32000 J/g; it is of interest as high energy density material[16]. Aluminium can induce thermite reaction with MnO_2 nanoparticles; this binary mixture can secure solid particles at high reaction temperature [6]. Nitrocellulose (NC) is the most common energetic polymeric binder; NC can offer gaseous products of 871 l/kg and explosion heat of 4312 kJ/kg [17]. NC can be employed as energetic binder for advanced electric match compositions [18]. These features can offer enhanced propagation index (PI). PI is a simple method to assess mixture's tendency to sustain burning upon initial ignition by an external stimulus (Equation 1) [9].

$$PI = \Delta H_{reaction} / T_{ignition} \qquad (1)$$

Compositions with high reaction enthalpy and low ignition temperature can secure self sustained propagation at high rate. NC has recently been employed to modify some energetic

material; NC was employed as energetic coating for Al/CuO nanoparticles for underwater ignition [19-21]. Nanothermite particles can offer vigorous exothermic reaction, with high gravimetric heat output compared with conventional explosives [22-24]. These novel characteristics inspire us to utilize NC as energetic binder for colloidal nanothermite particles. MnO_2 nanoparticles of 10 nm were developed using hydrothermal synthesis. Aluminum nanoparticles of 100 nm particle size were developed by wet milling. MnO_2/Al nanoparticles were re-dispersed in acetone; NC was dissolved in acetone colloid. MnO_2/Al/NC nanocopmosite was developed via co-precipitation. Uniform distribution of nanothermite particles into NC was verified via SEM and elemental mapping. The impact of nanothermite particles on NC thermal behaviour was evaluated using DSC and TGA. Nanothermite particles offered an increase in total heat release by 150 %, with decrease in ignition temperature by 8 ^{0}C. Propagation index was enhanced by 261 %. Main decomposition kinetic parameters were investigated using Kissinger and KAS models. Nanothermite particles experienced drastic decrease in NC activation energy by 10 % using Kissinger and KAS models.

2. Experimental

2.1 Synthesis of MnO_2 nanoparticles

MnO_2 particles were manufactured using hydrothermal processing. Nanoparticles were fabricated in continuous manner via direct mixing of metal salt with supercritical fluid. Schematic for continuous hydrothermal synthesis is provided (Figure S1). Further details about hydrothermal synthesis can be found in the following references [5, 22, 24]. Nano-oxide particles were flocculated from their synthesis medium and re-dispersed in organic solvent with aluminium nanoparticles.

2.2 Development of NC nanocomposite

Nanoparticles have natural tendency to aggregate with decrease in their surface area [25]. Enhanced dispersion characteristics could be accomplished via integration of dispersed particles into energetic matrix [5, 25]. Stoichiometric binary mixture of MnO_2/Al nanoparticles was re-dispersed into acetone; consequently NC was dissolved in acetone colloid. The hybrid nanocomposite material was developed via co-precipitation technique (Figure 2).

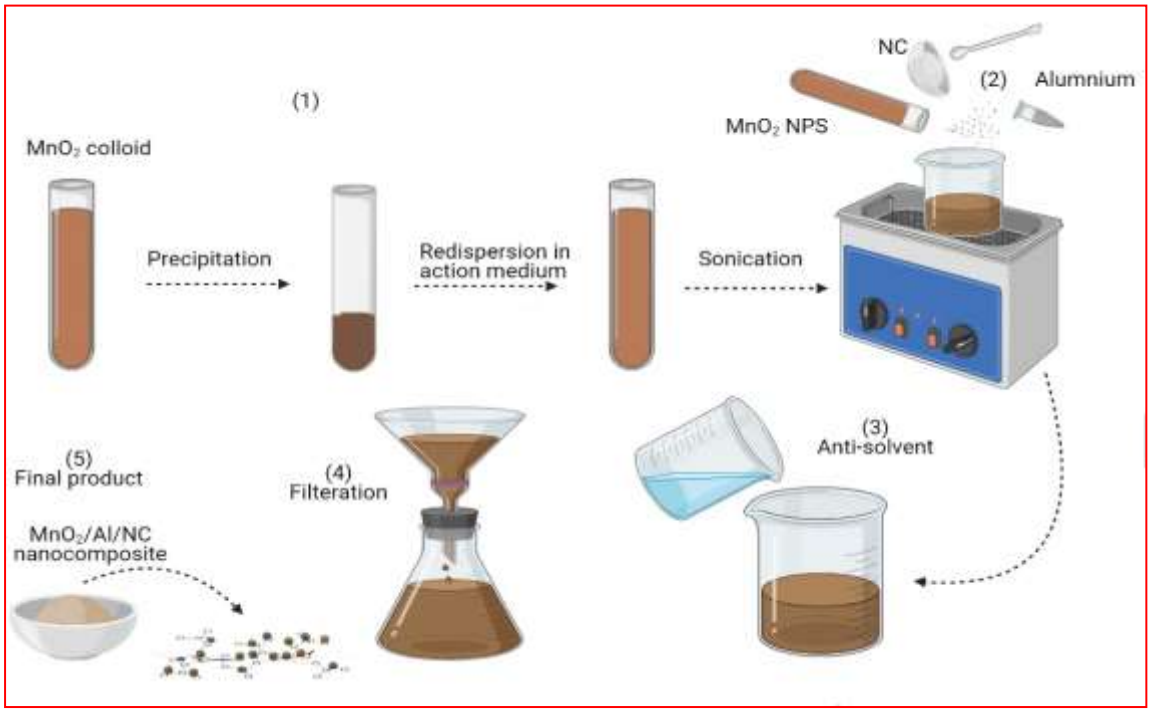

Fig. 2: Schematic for integration of colloidal nanothermite particles into NC via co-precipitation technique.

2.3 Characterization of NC nanocomposite

Size and shape of synthesized nanothermite particles were investigated using TEM (JEM-2100F by Joel Corporation). Morphology of dry particles was investigated with SEM, ZEISS SEM EVO 10 MA. Morphology of developed NC nanocomposite was investigated with SEM; elemental distribution of nanothermite particles into energetic matrix was investigated with EDAX detector.

2.4 Thermal behaviour of NC nanocomposite

Nanothermite particles can act as efficient high energy density material. Thermal behaviour of MnO_2/Al/NC nanocomposite was investigated using DSC Q200 by TA. The tested sample was heated up to 500 ^{0}C, at 5 ^{0}C min^{-1}. MnO_2/Al/NC weight loss was with temperature was further assessed using TGA 55 by TA.

2.5 Kinetics analysis

Kinetic analysis is vital to assess the main decomposition parameters including: pre-exponential factor (A), kinetic model (f(α)), and activation energy (Ea) [26-27]. The impact of nanothermite particles on NC decomposition kinetic was assessed using TGA. The weight loss of tested sample was recorded at different heating rates 2, 4, 6, 8 and 10°C·min^{-1}. Kissinger and Kissinger–Akahira–Sunose (KAS) were adopted for kinetic analysis.

2.5.1 Activation energy calculation

Activation energy (Ea) can be evaluated from Kissinger's model (Equation 2)

$$-\frac{Ea}{R} = \frac{d\ln(\beta/T_p^2)}{d(1/T_p)} \quad (2)$$

Where β, and Tp are the heating rate, and peak temperature at that heating rate respectively [28-29]. Furthermore, precise evaluation of activation energy (E_a) can be accomplished by Kissinger–Akahira–Sunose (KAS) (Equation 3) [30].

$$\ln\left(\frac{\beta_i}{T_{\alpha,i}^{1.92}}\right) = Const - 1.0008\frac{E\alpha}{RT\alpha} \quad (3)$$

3. Results and discussions

3.1 Characterization of nanothermite particles

TEM micrographs revealed mono-dispersed MnO_2 particles of 10 nm average particle size (Figure 3-a); lattice diffraction pattern confirmed mono-crystalline structure (Figure 3-b).

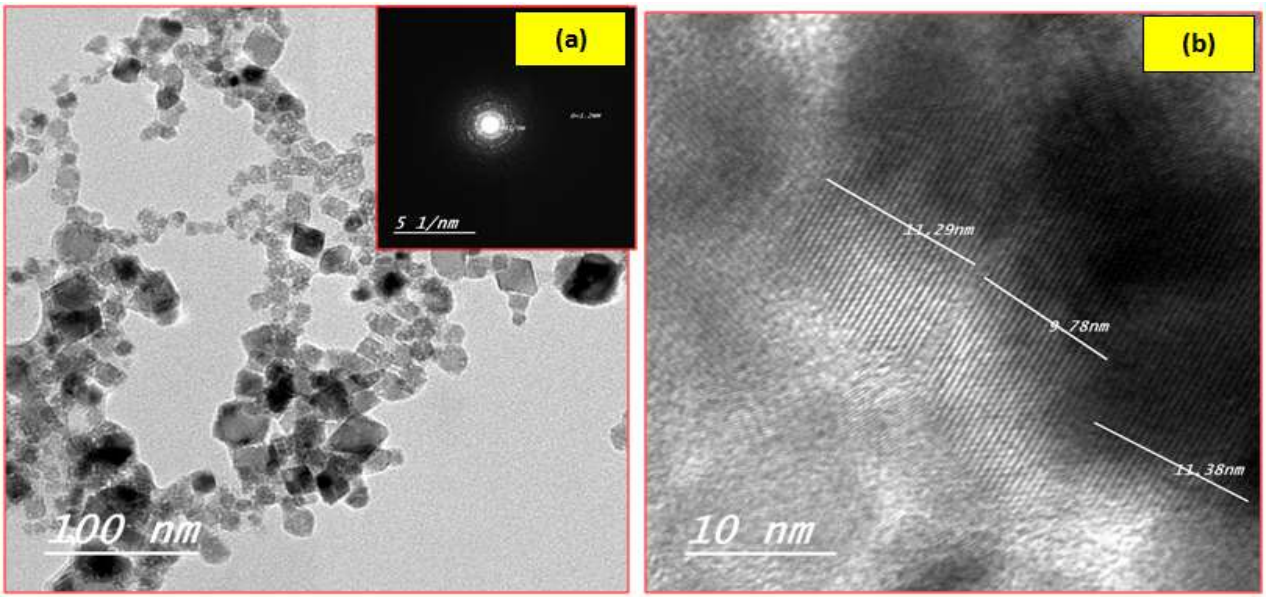

Fig. 3: TEM micrograph of fabricated MnO_2 nanocatalyst (a), lattice crystalline structure (b).

Morphology of MnO_2 particles was investigated with SEM; SEM micrographs emphasis the high tendency of MnO_2 particles to decrease their number over drying process (Figure 4) [31-34].

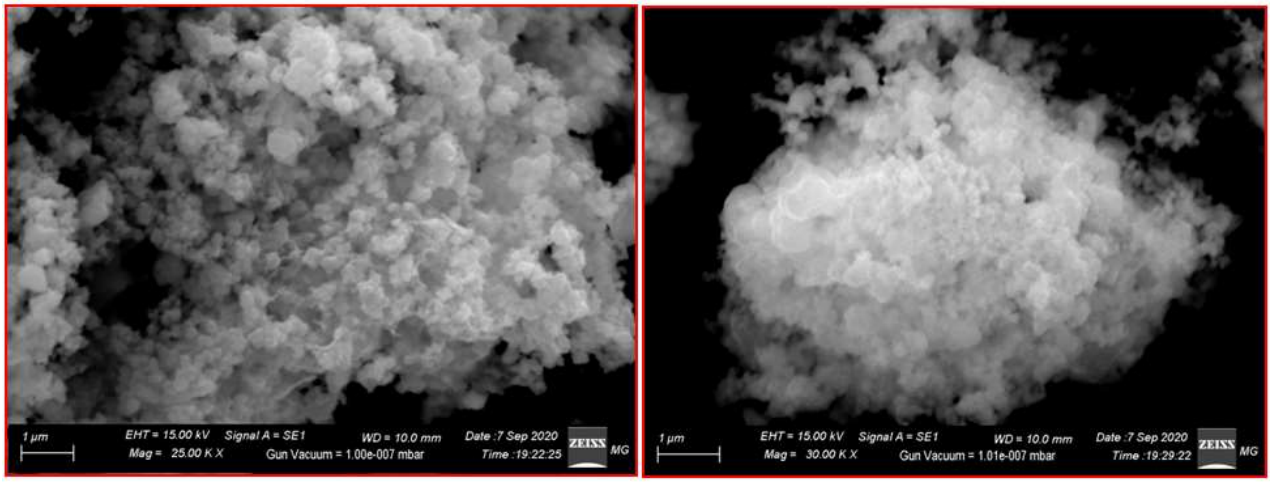

Fig. 4: SEM micrographs of dry MnO_2 nanocatalyst.

Elemental mapping confirmed stochiometrically balanced MnO_2 composition with uniform elemental distribution of Mn, and O (Figure 5).

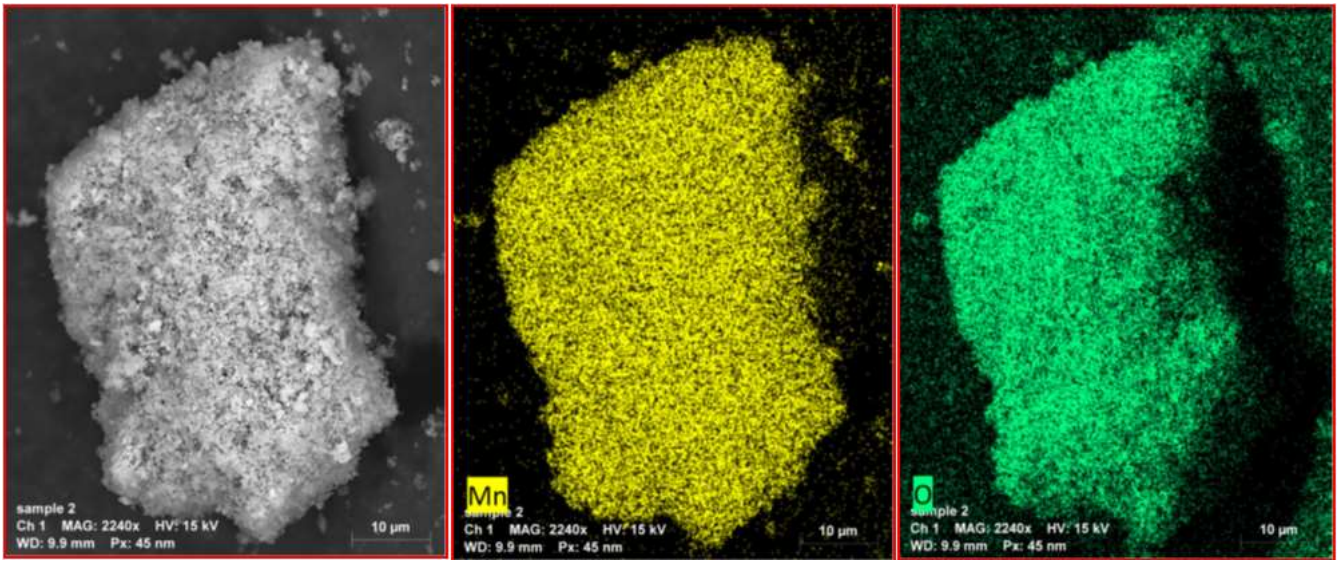

Fig. 5: Elemental mapping of synthesized MnO_2 nanocatalyst.

TEM micrographs of aluminum particles demonstrated nanoplates of 100 nm average particle size (Figure 6-a). Incident beam diffraction demonstrated highly crystalline structure (Figure 6-b).

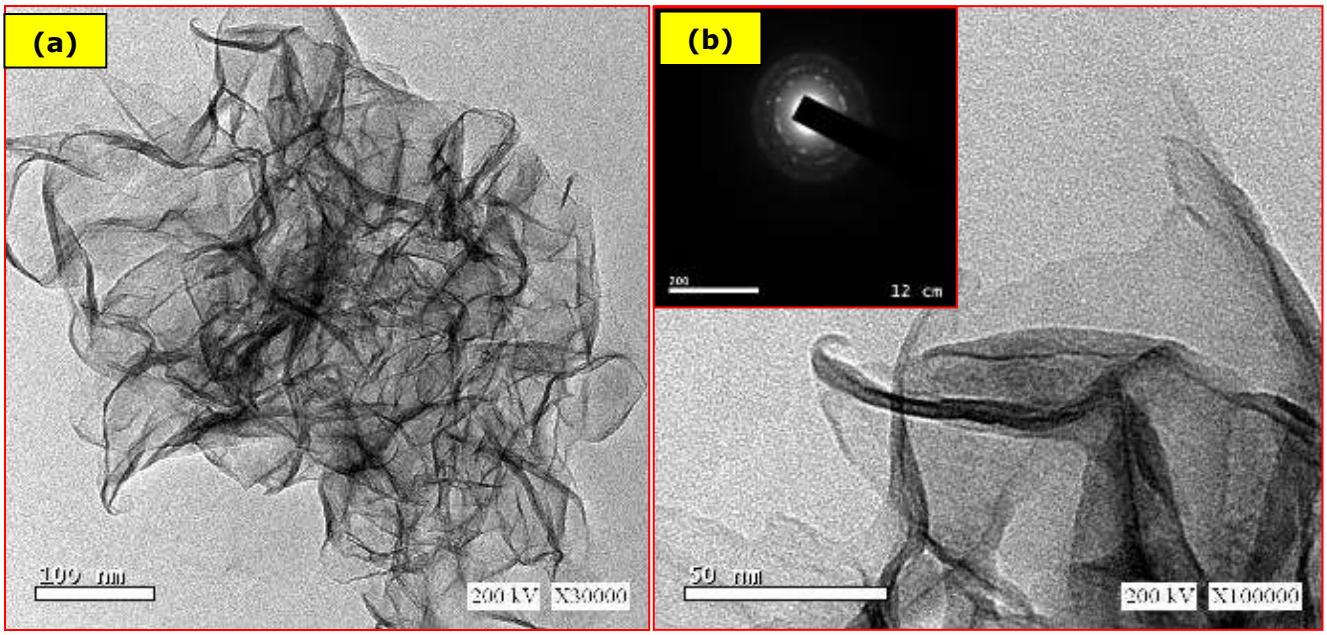

Fig. 6: TEM micrographs of aluminum nanoparticles.

3.2 Characterization of NC nanocomposites

Incorporation of colloidal particles into energetic matrix can secure enhanced levels of particle dispersion [35-37]. Enhanced particle (metal oxide/metal) dispersion is mandatory for high reaction rate, and heat release rate. Morphology of dry NC nanocomposite was investigated with SEM. SEM

micrographs demonstrated NC fibres with 20 µm diameter (Figure 7-a), with uuniform dispersion of nanothermite particles into energetic matrix (Figure 7-b).

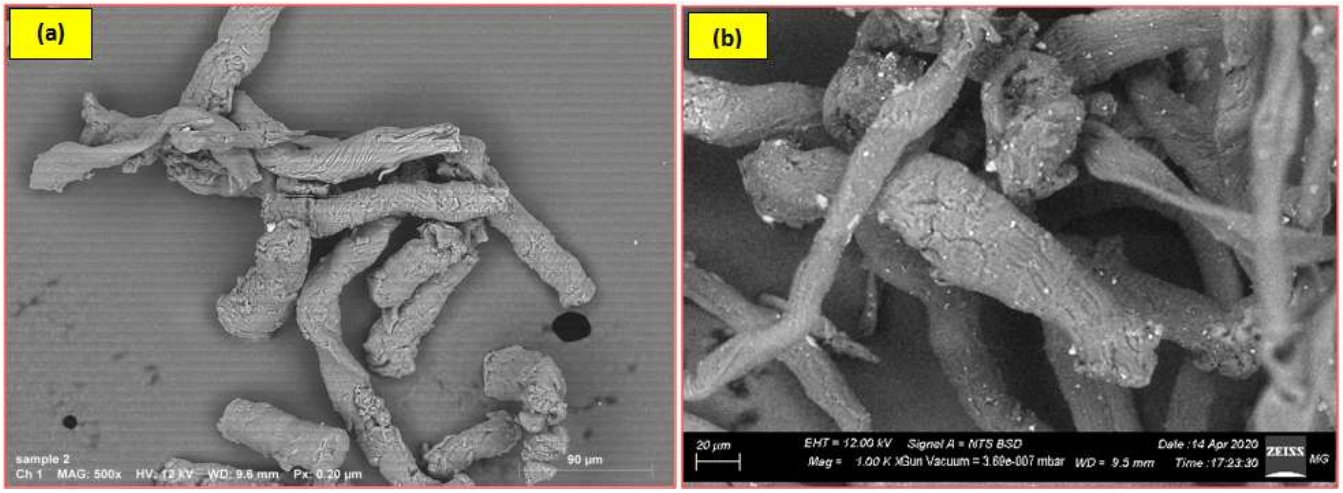

Fig. 7: SEM micrographs of NC (a), MnO_2/Al/NC nanocomposite (b).

Elemental mapping (using EDX detector) confirmed uniform dispersion of nanothermite particles into NC matrix (Figure 8).

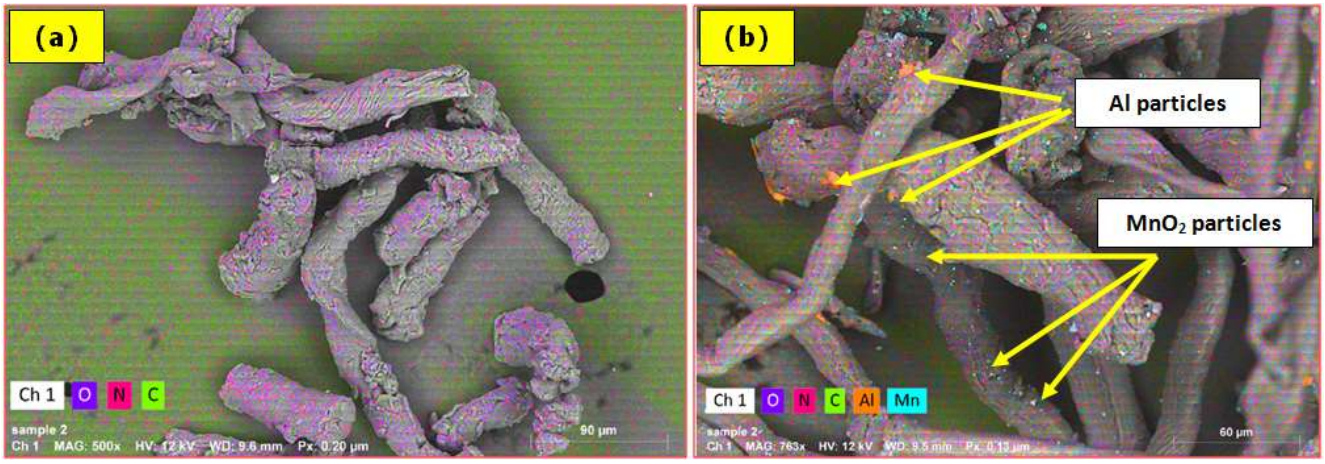

Fig. 8: Elemental mapping for of NC (a), MnO_2/Al/NC nanocomposite (b).

Iintegration of colloidal nanothermite particles into NC matrix demonstrated uniform particle dispersion.

3.3 Thermal behaviour of NC nanocomposite

Nanothermite particles offered an increase in NC total heat release by 150 %, with decrease in ignition temperature by 8 ^{0}C using DSC (Figure 9). The surge increase in total heat release can offer enhanced ignitability and self-sustained reaction at high propagation rate.

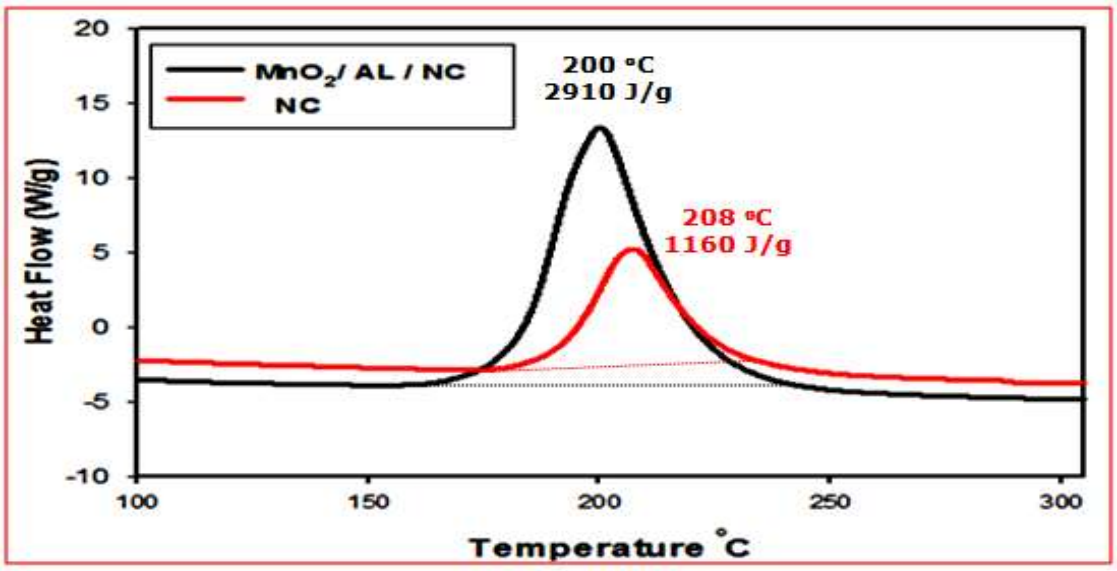

Fig. 9: DSC thermogram for NC and MnO_2/Al/NC nanocomposite.

MnO_2/Al/NC demonstrated enhanced propagation index by 261 % (Equation 1); enhanced propagation was ascribed to enhanced nanothermite particle into the energetic matrix. Nanothermite particles can secure vigorous exothermic reaction with the release of solid oxide as high temperature. These characteristics can inherit novel characteristics for electric match and ignition compositions. TGA analysis (Figure 10) confirmed DSC out comess; MnO_2/Al/NC demonstrated decrease in main decomposition temperature by 8 ^{0}C compared with NC.

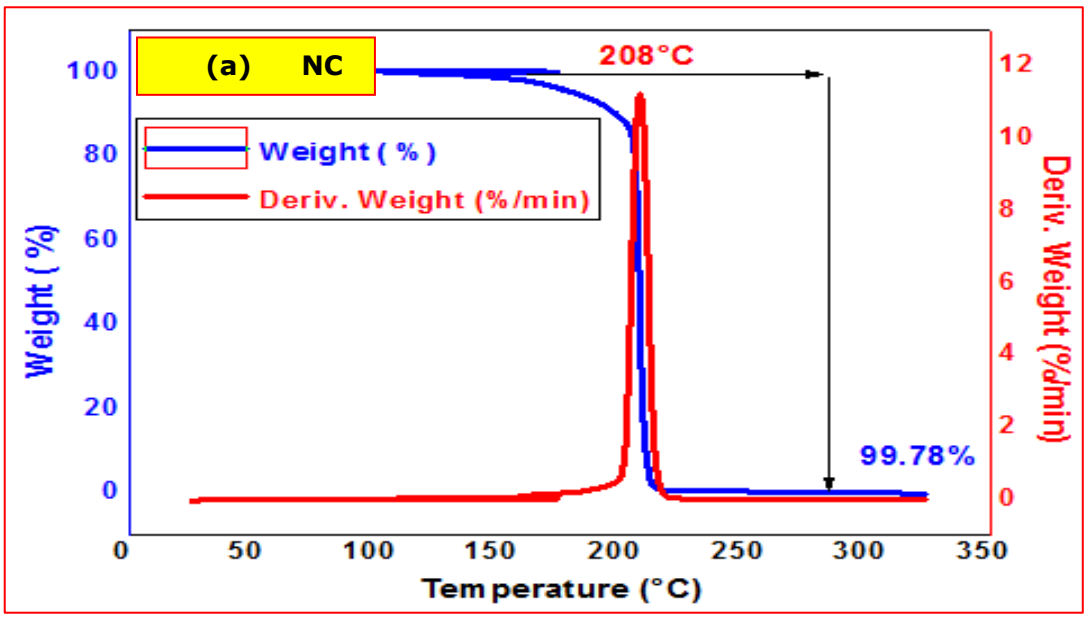

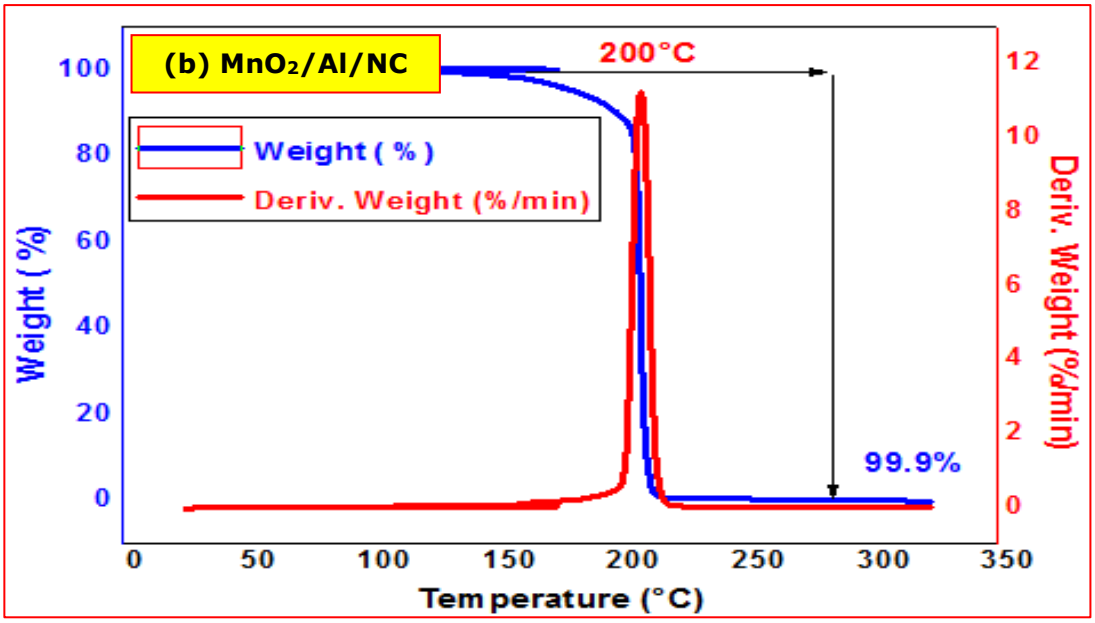

Fig. 10: TGA thermogram of NC (a), and MnO_2/Al/NC nanocomposite (b).

3.4 Decomposition kinetics of NC nanocomposite

3.4.1 Kinetic parameters via Kissinger model

The impact of nanothermite particles on NC kinetic decomposition was investigated using nonisothermal technique. MnO_2/Al/NC nancomposite was investigated using TGA; weight loss was investigated at four different heating rates of 2, 4, 6, 8 and 10 °C·min^{-1} (Figure 11).

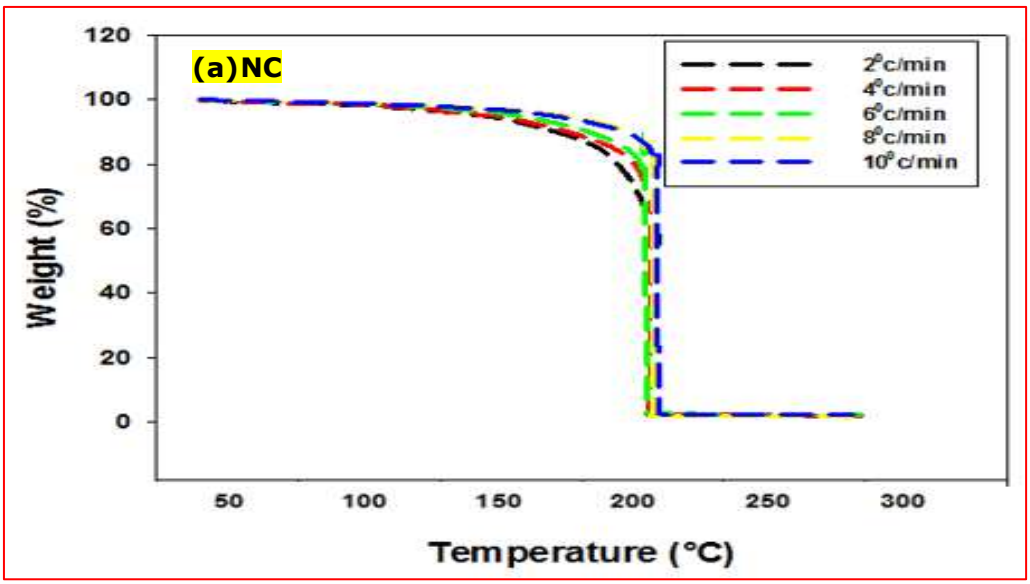

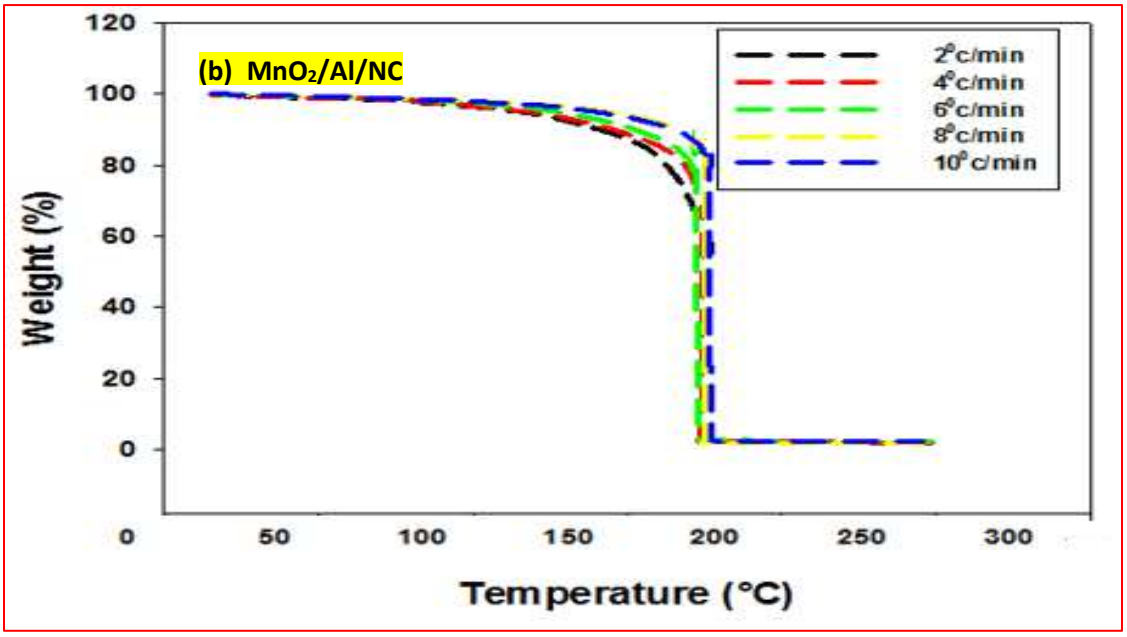

Fig. 11: TGA thermograms of NC (a), MnO_2/Al/NC nanocomposite (b)

The activation energy of MnO_2/Al/NC nanocomposite was evaluated to NC; activation energy was obtained from the slop of the straight line by plotting $\ln(\beta/T^2)$ versus (1/T) at the five heating rates (Figure 12).

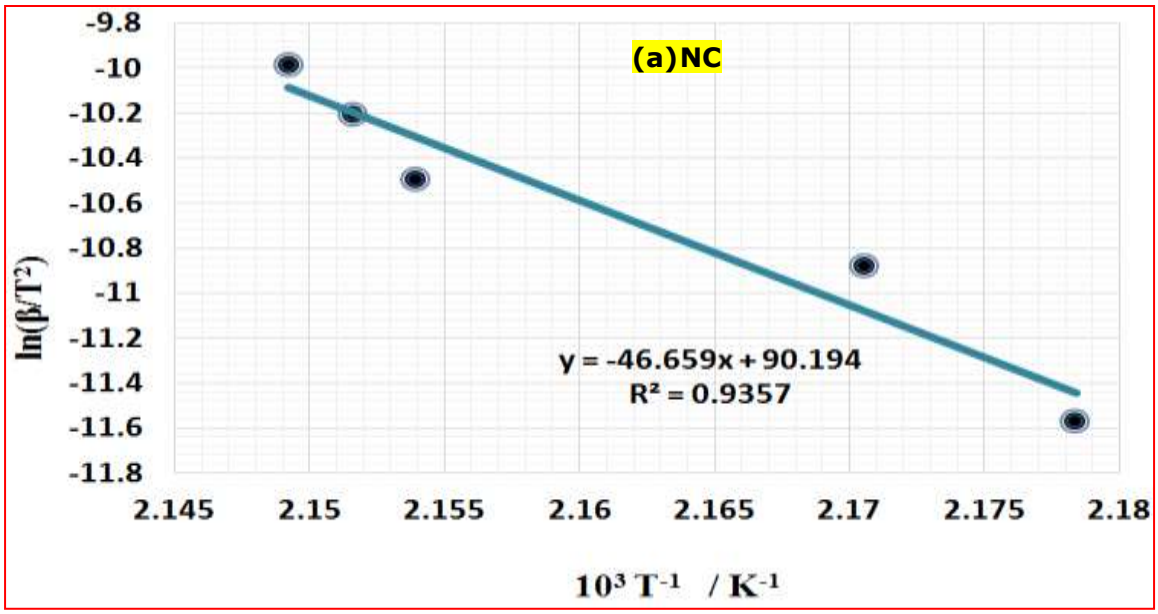

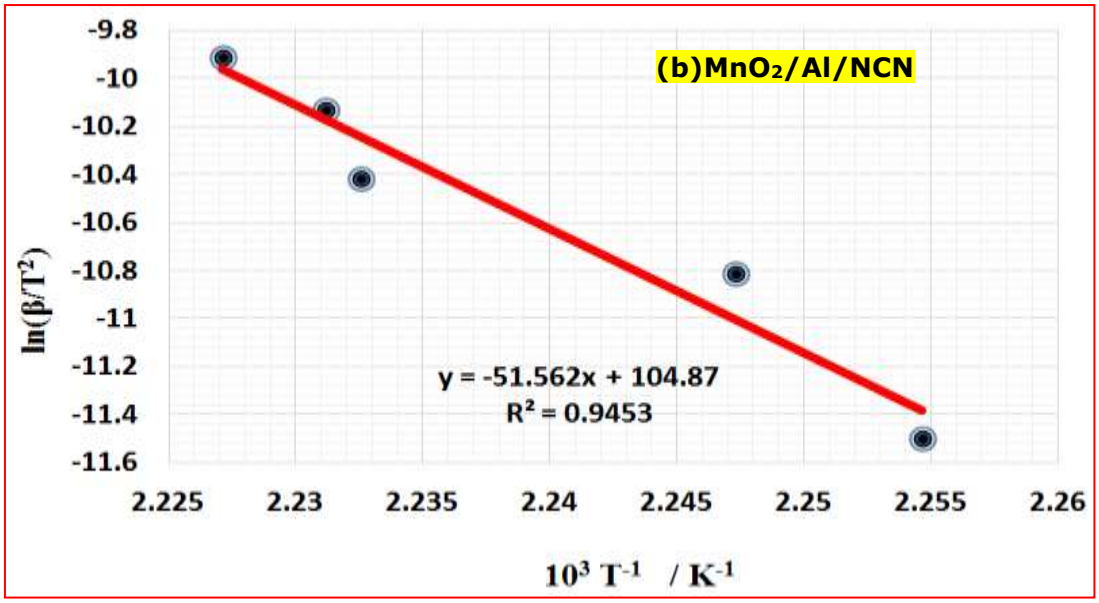

Fig. 12: Kissinger method to determine the activation energy of NC (a), MnO_2/Al/NC (b).

While NC experienced mean activation energy of 430 KJ·mol^{-1}; MnO_2/Al/NC nanocomposite demonstrated mean activation of 388 KJ·mol^{-1}. MnO_2 particles with negative oxygen surface and hydrous surface can act as efficient catalyst with decrease in activation enenrgy [7-8, 13].

3.4.2 Kinetic parameters via KAS model

The activation energy at the different fractional conversion was determined by using modified Kissinger–Akahira–Sunose (KAS) method. The kinetics parameters of NC and MnO_2/Al/NC are tabulated in Table 1.

Table 1: Kinetic parameters of MnO_2/Al/NC nanocomposite using (KAS) model to pure NC.

α reacted	NC			MnO_2/Al/NC nanocomposite		
	Ea (kJ mol^{-1})	Log A (s^{-1})	r	Ea (kJ mol^{-1})	Log A (s^{-1})	r
0.05	420	50	0.982	380	43	0.992
0.1	418	51	0.993	381	42	0.995
0.15	417	52	0.987	379	41	0.982
0.2	420	53	0.989	378	40	0.982
0.25	421	50	0.992	381	42	0.984
0.3	418	51	0.982	380	41	0.994

0.35	419	52	0.998	381	42	0.988
0.4	420	51	0.995	378	41	0.997
0.45	421	50	0.996	379	43	0.996
0.5	422	52	0.988	379	42	0.998
0.55	421	51	0.996	380	41	0.983
0.6	420	52	0.985	381	42	0.986
0.65	422	51	0.998	382	42	0.996
0.7	423	52	0.998	378	43	0.998
0.75	420	53	0.999	380	41	0.986
0.8	421	51	0.988	381	40	0.986
0.85	421	52	0.999	382	43	0.995
0.9	420	51	0.999	380	44	0.997
Mean	**420**	**50**		**380**	**43**	

The mean value of the activation energies of NC and MnO_2/Al/NC nanocomposite was 420 kJ·mol^{-1} and 380 kJ·mol^{-1} respectively. These findings confirmed results from Kissinger's model.

4. Conclusion and future work

MnO_2/Al can secure one of the most vigorous nanothermite reactions in terms of heat output, gaseous products. Mono-dispersed MnO_2 particles of 10 nm particle size were developed by hydrothermal synthesis. Aluminium nanoplates of 100 nm were adopted. Integration of colloidal nanothermite particles into nitrocellulose offered enhanced dispersion characteristics. Consequently high interfacial surface area, high heat release rate can be achieved. Nanothermite particles offer an increase in NC heat output by 150 %; additionally the ignition temperature was decreased by 8 ^{0}C. Nanothermite particles offered an enhanced propagation index of NC by 261. Additionally, nanothermite particles offered decrease in NC activation energy by 10 %. It can be concluded that nanothermite particles can act as catalyst and high energy density material due to synergism between aluminium and MnO_2 nanoparticles.

Reference

1. *Jian, G., et al., Nanothermite reactions: Is gas phase oxygen generation from the oxygen carrier an essential prerequisite to ignition? Combustion and Flame, 2013.* ***160****(2): p. 432-437.*
2. *Shin, D.J., et al., Nanothermite of Al nanoparticles and three-dimensionally ordered macroporous CuO: Mechanistic insight into oxidation during thermite reaction. Combustion and Flame, 2018.* ***189****: p. 87-91.*
3. *Comet, M., et al., Nanothermite foams: From nanopowder to object. Chemical Engineering Journal, 2017.* ***316****: p. 807-812.*
4. *Elbasuney, S. and M. Yehia, Ferric Oxide Colloid: A Novel Nano-catalyst for Solid Propellants. Journal of Inorganic and Organometallic Polymers and Materials, 2020.* ***30****(3): p. 706-713.*
5. *Elbasuney, S., et al., Stabilized super-thermite colloids: A new generation of advanced highly energetic materials. Applied Surface Science, 2017.* ***419****: p. 328-336.*
6. *Elbasuney, S., et al., Novel (MnO2/Al) thermite colloid: an opportunity for energetic systems with enhanced performance. Journal of Materials Science: Materials in Electronics, 2020.* ***31****(23): p. 21399-21407.*
7. *Elbasuney, S. and M. Yehia, Thermal decomposition of ammonium perchlorate catalyzed with CuO nanoparticles. Defence Technology, 2019.* ***15****(6): p. 868-874.*
8. *Elbasuney, S. and M. Yehia, Ammonium Perchlorate Encapsulated with TiO2 Nanocomposite for Catalyzed Combustion Reactions. Journal of Inorganic and Organometallic Polymers and Materials, 2019.* ***29****(4): p. 1349-1357.*
9. *CONKLING, J. and C. MOCELLA, eds. Chemistry of Pyrotechnics Basic Principles and Theory. Second ed. 2012, CRC: London.*
10. *Benhammada, A., et al., Synthesis and characterization of α-Fe2O3 nanoparticles from different precursors and their catalytic effect on the thermal decomposition of nitrocellulose. Thermochimica Acta, 2020.* ***686****: p. 178570.*
11. *HAAG, W.O., B.C. GATES, and H.K. ZINGER, eds. ADVANCES IN CATALYSIS. Vol. 44. 2000, ACADEMIC PRESS: San Diego.*
12. *Elbasuney, S., et al., Ferric oxide colloid: novel nanocatalyst for heterocyclic nitramines. Journal of Materials Science: Materials in Electronics, 2021.*
13. *Elbasuney, S. and G.S. El-Sayyad, The potentials of TiO2 nanocatalyst on HMX thermolysis. Journal of Materials Science: Materials in Electronics, 2020.* ***31****(17): p. 14930-14940.*
14. *Elbasuney, S., et al., Multi-component nanocomposite infrared flare with superior infrared signature via synergism of nanothermite and reduced graphene oxide. Journal of Materials Science: Materials in Electronics, 2020.* ***31****(14): p. 11520-11526.*
15. *Elbasuney, S., et al., Facile synthesis of RGO-Fe2O3 nanocomposite: A novel catalyzing agent for composite propellants. Journal of Materials Science: Materials in Electronics, 2020.* ***31****(23): p. 20805-20815.*
16. *Elbasuney, S., Steric Stabilization of Colloidal Aluminium Particles for Advanced Metalized-Liquid Rocket Propulsion Systems. Combustion, Explosion, and Shock Waves, 2019.* ***55****(3): p. 353-360.*
17. *Meyer, R., J. Kohler, and A. Homburg, eds. EXPLOSIVES. Sixth ed. 2007, WILEY: Weinheim.*
18. *Dai, J., et al., Facile formation of nitrocellulose-coated Al/Bi2O3 nanothermites with excellent energy output and improved electrostatic discharge safety. Materials & Design, 2018.* ***143****: p. 93-103.*

19. *Kim, J.H., et al., Thermal reactions of nitrocellulose-encapsulated Al/CuO nanoenergetic materials fabricated in the gas and liquid phases. Materials Chemistry and Physics, 2019.* ***238****: p. 121955.*
20. *Zhou, X., et al., Facile preparation and energetic characteristics of core-shell Al/CuO metastable intermolecular composite thin film on a silicon substrate. Chemical Engineering Journal, 2017.* ***328****: p. 585-590.*
21. *Zhang, X. and B.L. Weeks, Preparation of sub-micron nitrocellulose particles for improved combustion behavior. Journal of Hazardous Materials, 2014.* ***268****: p. 224-228.*
22. *Elbasuney, S., et al., Infrared Signature of Novel Super-Thermite (Fe2O3/Mg) Fluorocarbon Nanocomposite for Effective Countermeasures of Infrared Seekers. Journal of Inorganic and Organometallic Polymers and Materials, 2018.* ***28****(5): p. 1718-1727.*
23. *Elbasuney, S., et al., Infrared Spectra of Customized Magnesium/Teflon/Viton Decoy Flares. Combustion, Explosion, and Shock Waves, 2019. 55(5).*
24. *Elbasuney, S., et al., Super-Thermite (Al/Fe2O3) Fluorocarbon Nanocomposite with Stimulated Infrared Thermal Signature via Extended Primary Combustion Zones for Effective Countermeasures of Infrared Seekers. Journal of Inorganic and Organometallic Polymers and Materials, 2018.* ***28****.*
25. *Elbasuney, S., Dispersion characteristics of dry and colloidal nano-titania into epoxy resin. Powder Technology, 2014.* ***268****(0): p. 158-164.*
26. *Khawam, A. and D.R. Flanagan, Basics and applications of solid-state kinetics: a pharmaceutical perspective. Journal of pharmaceutical sciences, 2006.* ***95****(3): p. 472-498.*
27. *Trache, D., A. Abdelaziz, and B. Siouani, A simple and linear isoconversional method to determine the pre-exponential factors and the mathematical reaction mechanism functions. Journal of Thermal Analysis and Calorimetry, 2017.* ***128****(1): p. 335-348.*
28. *Vyazovkin, S., et al., ICTAC Kinetics Committee recommendations for performing kinetic computations on thermal analysis data. Thermochimica acta, 2011.* ***520****(1-2): p. 1-19.*
29. *Trache, D., et al., Physicochemical properties of microcrystalline nitrocellulose from Alfa grass fibres and its thermal stability. Journal of Thermal Analysis and Calorimetry, 2016.* ***124****(3): p. 1485-1496.*
30. *Akahira, T., Trans. Joint convention of four electrical institutes. Res. Rep. Chiba Inst. Technol., 1971.* ***16****: p. 22-31.*
31. *Elbasuney, S., et al., Novel High Energy Density Material Based on Metastable Intermolecular Nanocomposite. Journal of Inorganic and Organometallic Polymers and Materials, 2020.* ***30****(10): p. 3980-3988.*
32. *Elbasuney, S., et al., The significant role of stabilized colloidal ZrO2 nanoparticles for corrosion protection of AA2024. Environmental Nanotechnology, Monitoring & Management, 2019.* ***12****: p. 100242.*
33. *Elbasuney, S., et al., Synthesis of CuO-distributed carbon nanofiber: Alternative hybrid for solid propellants. Journal of Materials Science: Materials in Electronics, 2020.* ***31****(11): p. 8212-8219.*
34. *Elbasuney, S., M. Gobara, and M. Yehia, Ferrite Nanoparticles: Synthesis, Characterization, and Catalytic Activity Evaluation for Solid Rocket Propulsion Systems. Journal of Inorganic and Organometallic Polymers and Materials, 2019.* ***29****(3): p. 721-729.*
35. *Elbasuney, S., Novel colloidal molybdenum hydrogen bronze (MHB) for instant detection and neutralization of hazardous peroxides. TrAC Trends in Analytical Chemistry, 2018.* ***102****: p. 272-279.*

36. *Elbasuney, S., Novel multi-component flame retardant system based on nanoscopic aluminium-trihydroxide (ATH). Powder Technology, 2017.* ***305****: p. 538-545.*
37. *Elbasuney, S., Sustainable steric stabilization of colloidal titania nanoparticles. Applied Surface Science, 2017.* ***409****: p. 438-447.*

Figures

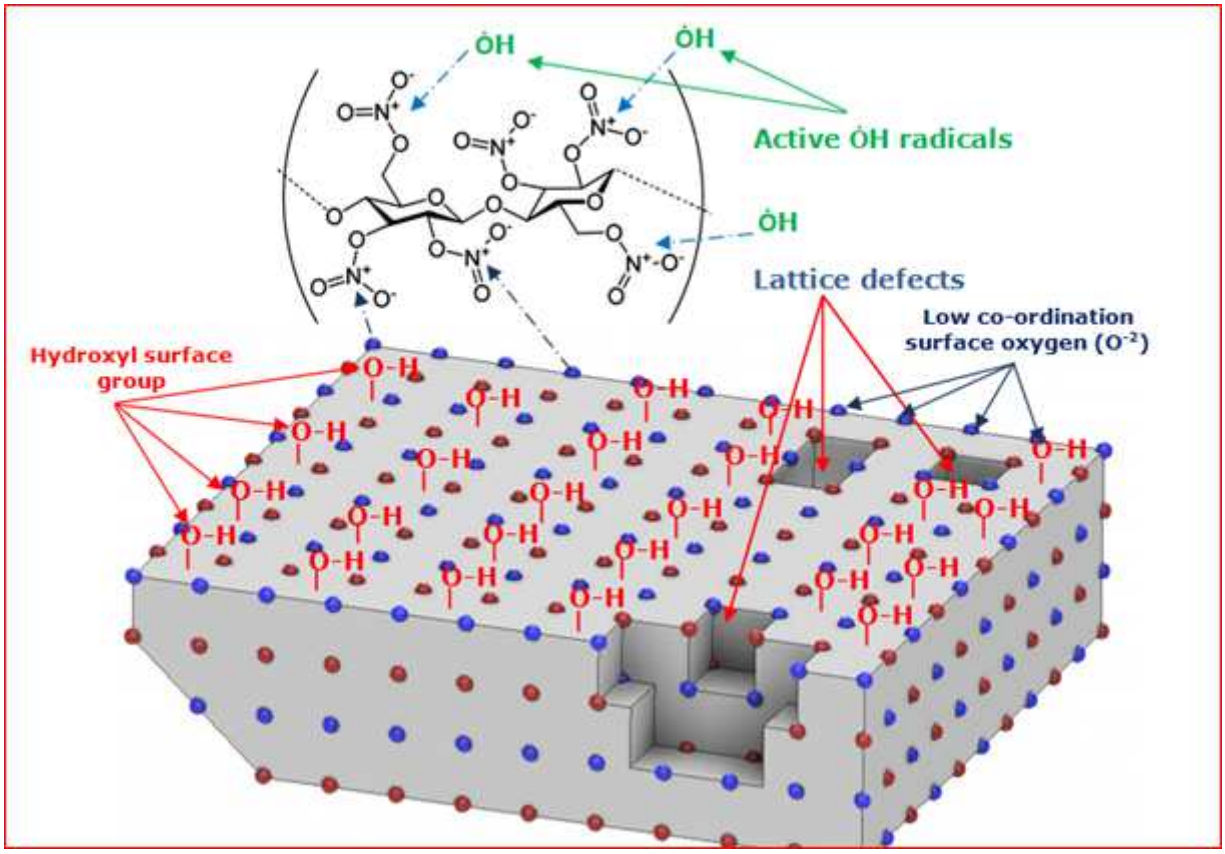

Figure 1

Schematic for active surface sites of manganese oxide catalyst (i. e. negative surface oxygen, and hydroxyl groups).

Figure 2

Schematic for integration of colloidal nanothermite particles into NC via co-precipitation technique.

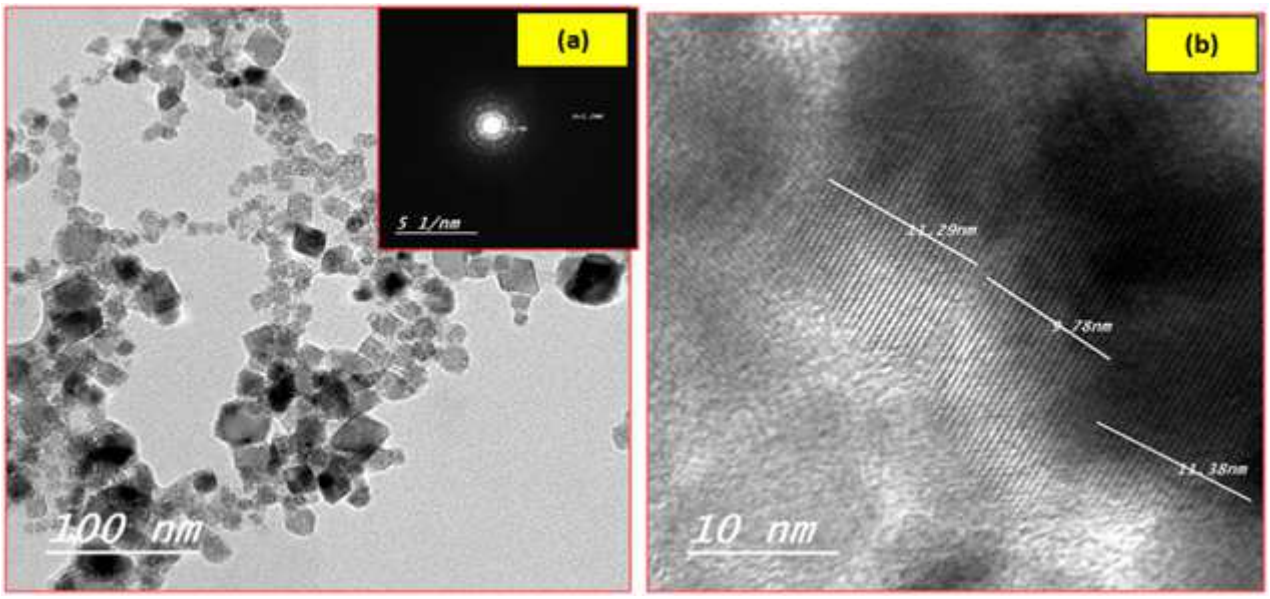

Figure 3

TEM micrograph of fabricated MnO2 nanocatalyst (a), lattice crystalline structure (b).

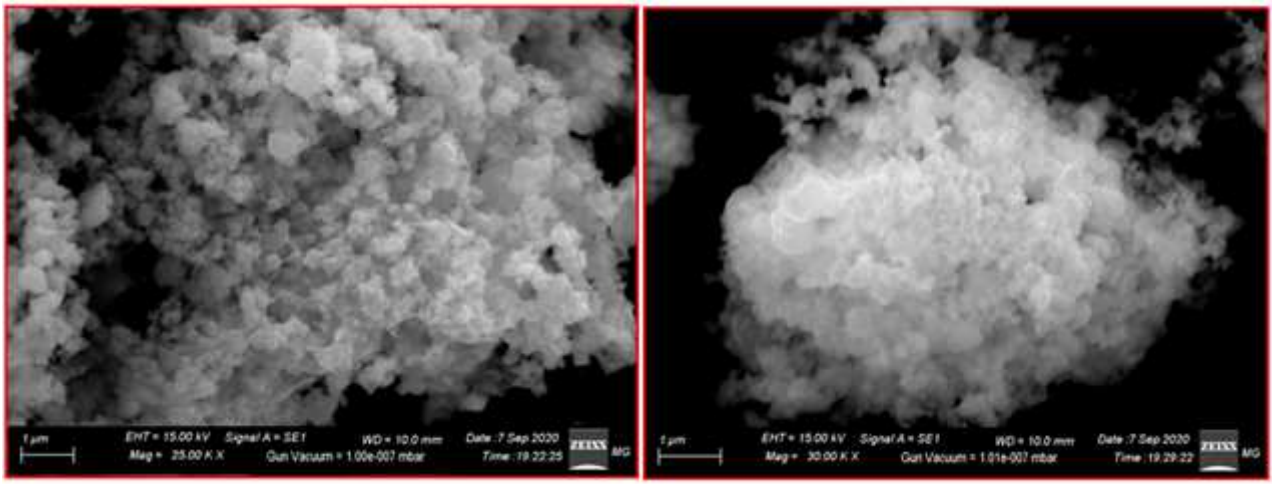

Figure 4

SEM micrographs of dry MnO2 nanocatalyst.

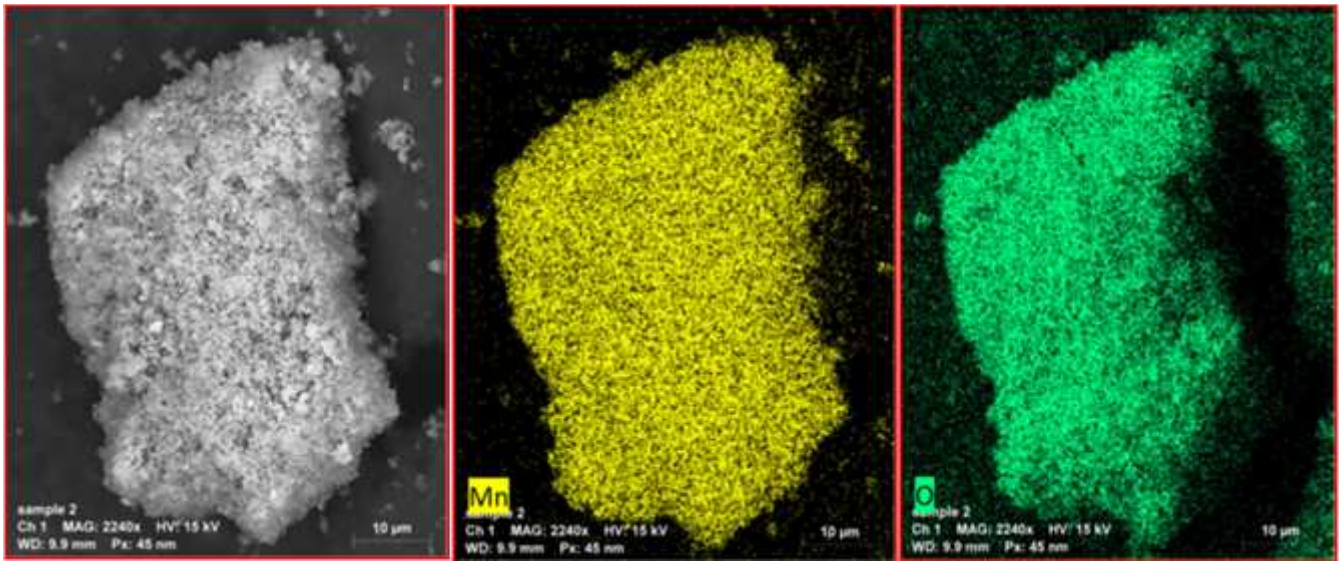

Figure 5

Elemental mapping of synthesized MnO2 nanocatalyst.

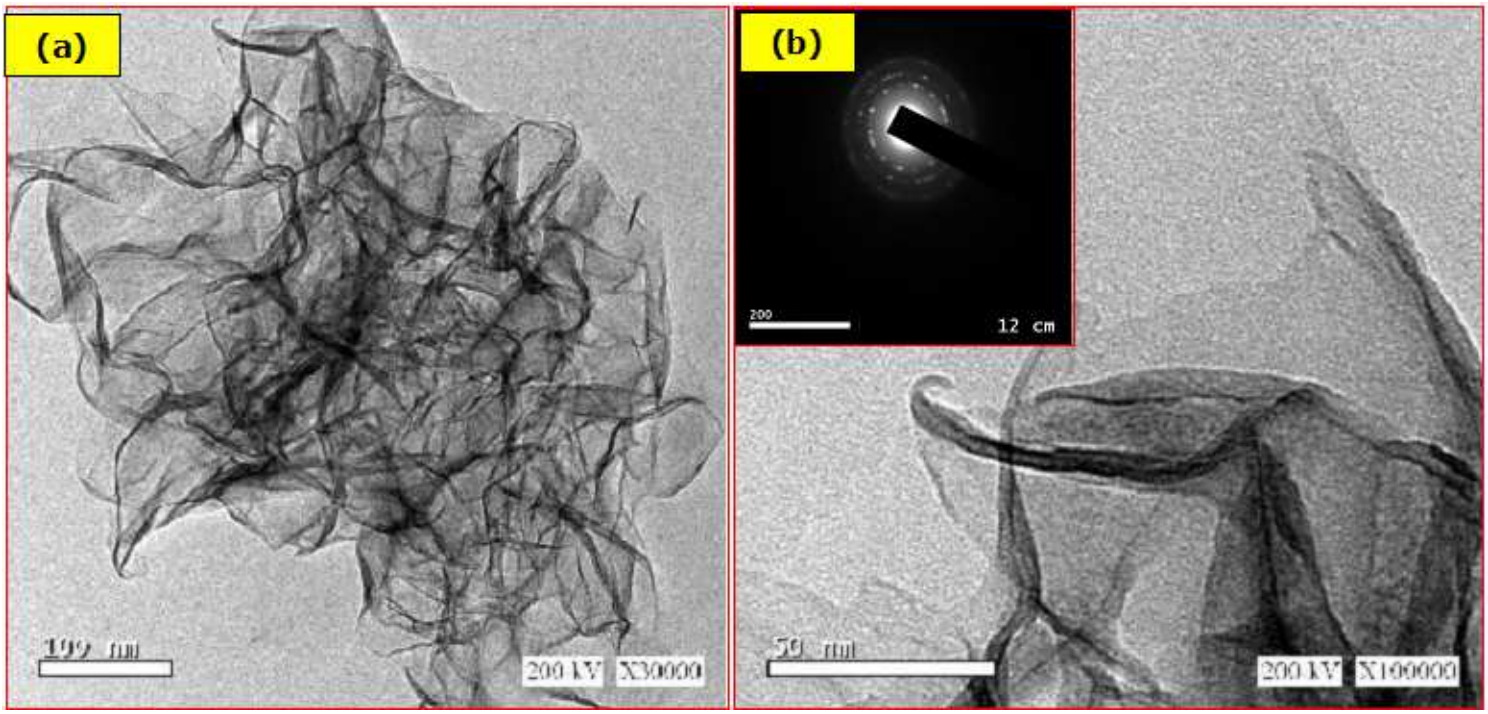

Figure 6

TEM micrographs of aluminum nanoparticles.

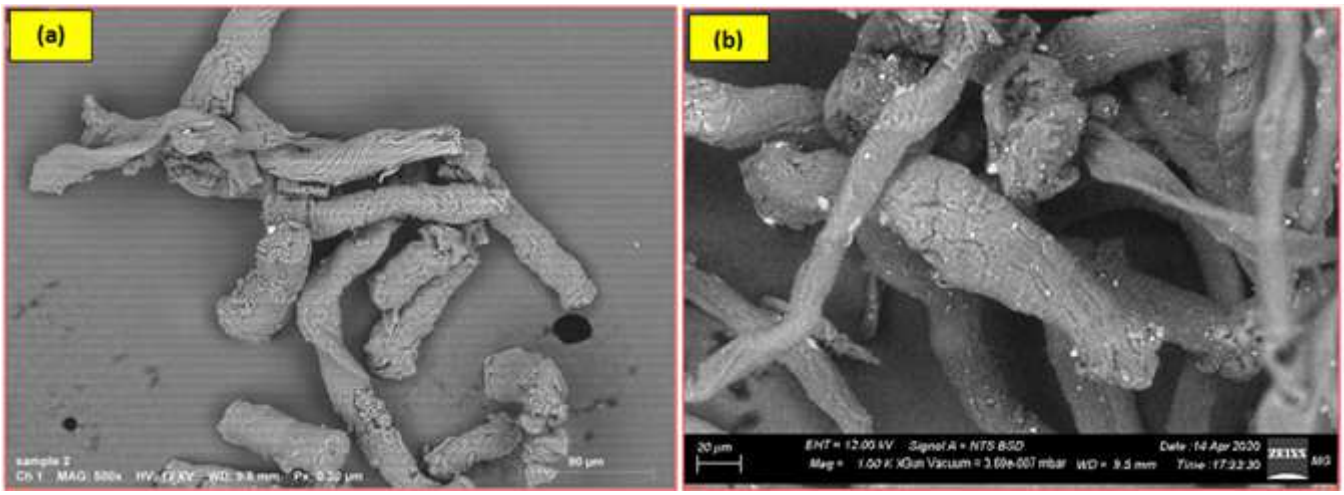

Figure 7

SEM micrographs of NC (a), MnO2/Al/NC nanocomposite (b).

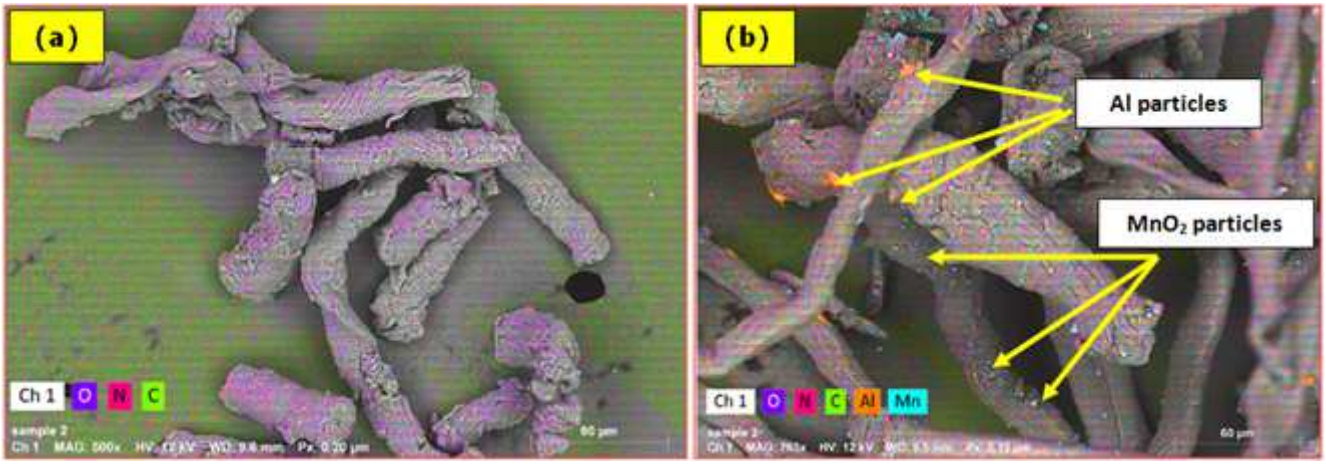

Figure 8

Elemental mapping for of NC (a), MnO2/Al/NC nanocomposite (b).

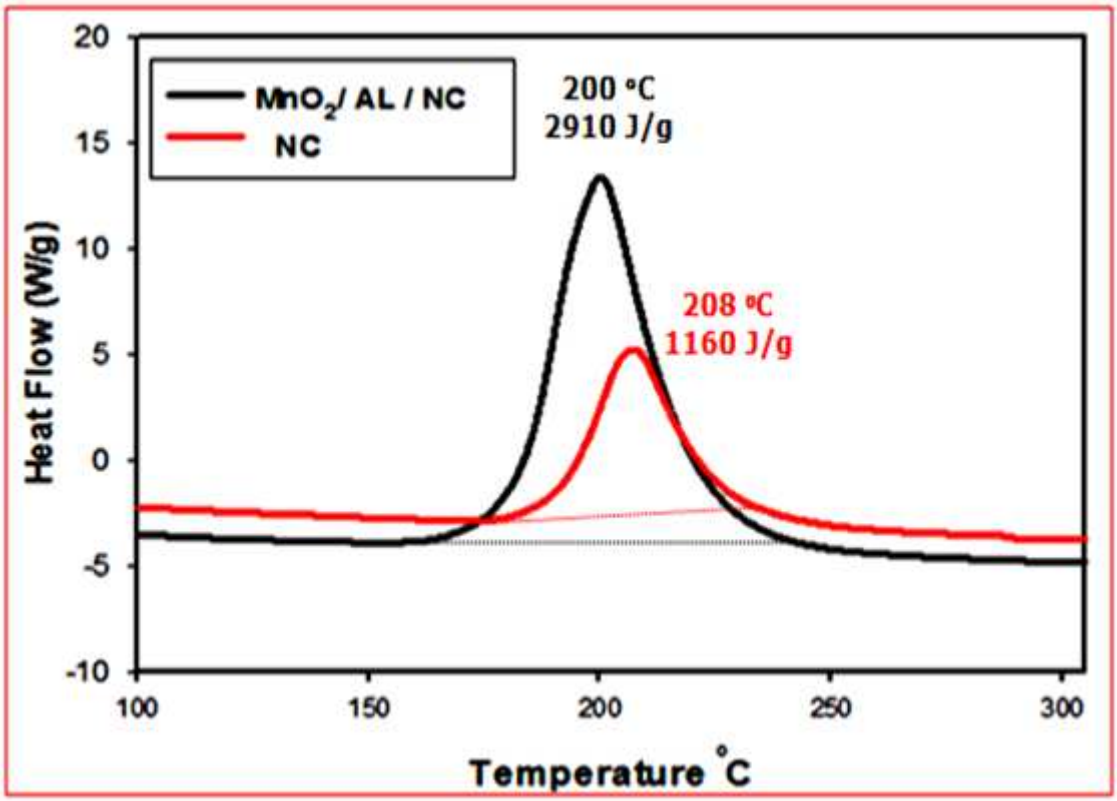

Figure 9

DSC thermogram for NC and MnO2/Al/NC nanocomposite.

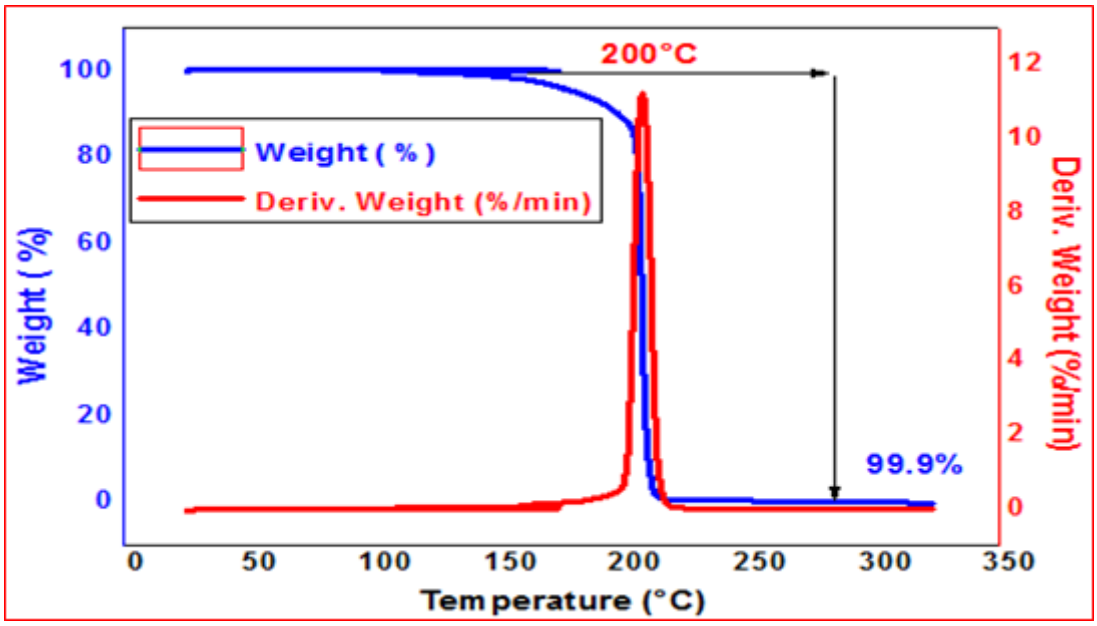

Figure 10

TGA thermogram of NC (a), and MnO2/Al/NC nanocomposite (b).

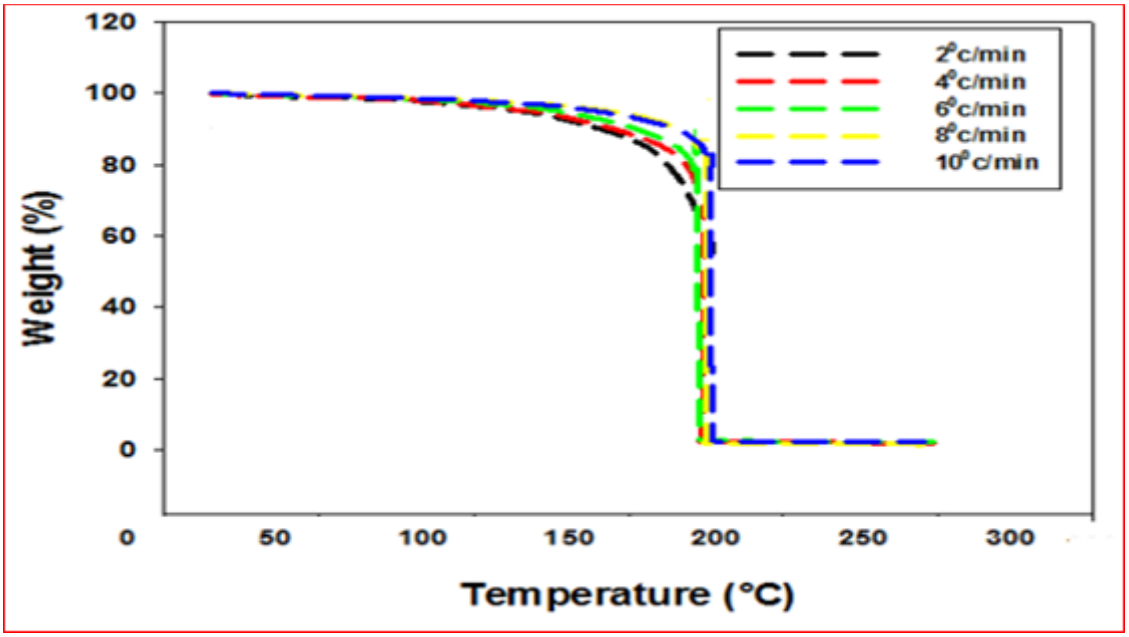

Figure 11

TGA thermograms of NC (a), MnO2/Al/NC nanocomposite (b)

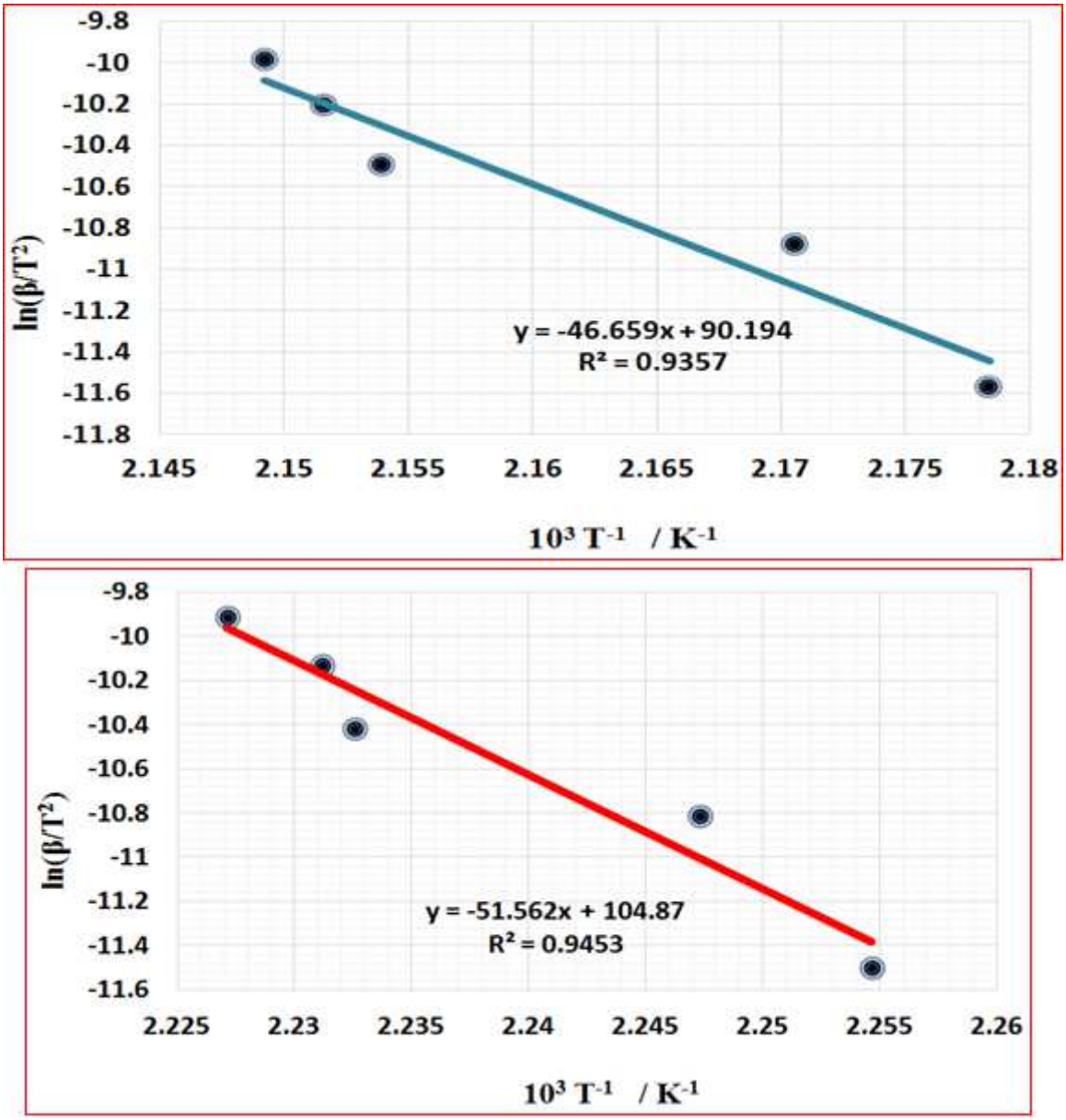

Figure 12

Kissinger method to determine the activation energy of NC (a), MnO2/Al/NC (b).